Electronic distributions in quasicrystalline $Al_{65}Cu_{20}Ru_{15}$ alloy

1996 J. Phys.: Condens. Matter 8 3513

(http://iopscience.iop.org/0953-8984/8/19/025)

J. Phys.: Condens. Matter **8** (1996) 3513–3523. Printed in the UK

Electronic distributions in quasicrystalline $Al_{65}Cu_{20}Ru_{15}$ alloy

Esther Belin-Ferré†, Zoltán Dankházi†‡, Anne Sadoc§, Claire Berger‖, Herbert Müller¶ and Hans Kirchmayr¶

† Laboratoire de Chimie Physique Matière et Rayonnement CNRS URA 176 and GDR CINQ, 11 rue Pierre et Marie Curie, 75231 Paris Cédex 05, France

‡ Institute for Solid State Physics, Muzéum krt 6-8, 1088 Budapest, Hungary

§ LURE, CNRS, MENESR, IP CEA, and GDR CINQ, Université Paris-Sud, 91405 Orsay Cédex, France and LPMS, 49 Avenue des Genottes, BP 8428, 95806 Cergy-Pontoise Cédex, France

‖ LEPES-CNRS and GDR CINQ, 25 Avenue des Martyrs, BP 166 X, 38042 Grenoble Cédex, France

¶ Institut für Experimentalphysik, Technical University Vienna, Wiedner Hauptstrasse 8–10, 1040 Wien, Austria

Received 20 October 1995, in final form 19 January 1996

Abstract. Occupied and unoccupied electronic distributions of quasicrystalline $Al_{65}Cu_{20}Ru_{15}$ have been studied mainly using soft-x-ray emission and absorption spectroscopy measurements. The partial distributions are adjusted in the binding energy scale in order to gain insight into the electronic interactions in this material. Interaction between Al states and Ru 4d states near the Fermi level and between Al and Cu 3d states in the middle of the occupied band is shown. At the Fermi level a significant pseudo-gap is observed in the Al 3p and 3s–d distributions. In the unoccupied band, the Ru and Cu d–s-like states are in interaction with the Al p states. The Ru and Cu states retain a slight d-like character at the energies of the conduction edges that suggests faint charge transfer to Ru atoms. Far from the Fermi level, the Ru and Cu states are strongly hybridized to s states. Adjustment of Al 3p and Al p distributions at the same intensity at the Fermi level points to a significant low intensity of the density of Al p conduction states over a few electronvolts from the Fermi level.

1. Introduction

Many stable icosahedral quasicrystals of great structural quality display high resistivities *a priori* unexpected for Al based intermetallics (see for example Klein *et al* 1991, Lanco *et al* 1992, Pierce *et al* 1993, Akimaya *et al* 1993, Basov *et al* 1994, Tamura *et al* 1994, Poon *et al* 1996). The Al densities of states (DOSs) at the Fermi level (E_F) of these alloys have been found to be significantly lower than those of pure fcc Al (Mori *et al* 1991, Belin *et al* 1992, Hippert *et al* 1992, Stadnik and Stroink 1993, Belin *et al* 1993, 1994, 1996). Quasicrystalline Al–Cu–Ru alloys have been reported to also exhibit very high resistivity values at low temperatures (Klein *et al* 1991, Poon 1992).

Theoretical densities of electronic states that could provide insight into the electronic properties of these alloys are still not available. Such calculations exist to date for several crystalline approximants (see for example Fujiwara and Yokokawa 1991, Fujiwara 1993, Fujiwara *et al* 1993, Krajci and Hafner 1993, Krajci *et al* 1995). Consequently,

† E-mail: belin@ccr.jussieu.fr.

0953-8984/96/193513+11$19.50

measurements of the electronic distributions of quasicrystals may supply information on their actual electronic structure, which may be helpful for understanding the physical and electronic properties.

Here, we report on an experimental investigation of the occupied and unoccupied band (OB and UB respectively) states distributions of single-phased quasicrystalline $Al_{65}Cu_{20}Ru_{15}$ alloy using the soft-x-ray spectroscopy (SXS) and photoemission spectroscopy (XPS) techniques. The paper is divided into three main sections: the principles of SXS and XPS are recalled in the next section, information is given on the experimental procedures in section 3 and the results are presented and discussed in section 4.

Table 1. Analysed x-ray transitions, states investigated, studied energy ranges, experimental techniques and widths of the inner level involved in the x-ray transition. Values of the widths of the inner levels are taken from the article by Krause and Oliver (1979).

X-ray transition	States investigated	Energy range (eV)	Technique	Width of the inner level (eV)
K β: OB $\rightarrow$ 1s	Al 3p	1550–1565	SXES	<0.1
Al $L_{2,3}$: OB $\rightarrow$ $2p_{3/2}$	Al 3s–d	55–75	SXES	0.45
Al Lα: OB $\rightarrow$ $2p_{3/2}$	Cu 3s–d	920–940	SXES	0.5
Ru Lβ_2: OB $\rightarrow$ $2p_{3/2}$	Ru 3s–d	2827–2847	SXES	2.0
Al K: 1s $\rightarrow$ UB	Al p	1555–1585	SXAS	<0.1
Cu L_{III}: $2p_{3/2}$ $\rightarrow$ UB	Cu s–d	930–950	SXAS	0.56
Ru L_{III}: $2p_{3/2}$ $\rightarrow$ UB	Ru s–d	2830–2850	SXAS	2.0
Cu K: 1s $\rightarrow$ UB	Cu p	8970–9000	SXAS	1.55
Ru K: 1s $\rightarrow$ UB	Ru p	22 110–22 140	SXAS	5.33

2. Experimental techniques

The soft-x-ray emission and absorption spectroscopy techniques, denoted SXES and SXAS respectively, are known to be well suited to investigate both OB and UB electronic distributions of a solid. The x-ray transitions are governed by dipole selection rules; consequently, they probe *separately* the OB and UB electronic distributions for a given s, p, ... *character* around each *atomic site* in a solid whether it is metallic or not, crystalline, amorphous, ... The emitted or absorbed intensities during the emission or absorption processes are proportional to $\mathcal{N}(\varepsilon) * \mathcal{L}(n, \ell)$ where $\mathcal{N}(\varepsilon)$ is the OB or UB DOS and $\mathcal{L}(n, \ell)$ is the energy width of the inner level that is involved in the x-ray transition; note that the x-ray transitions are also transition probability dependent but the corresponding matrix elements are usually constant or vary slowly against energy so they do not need to be accounted for. Thus, using the SXS techniques, information is gained on electronic distributions although no absolute DOS values are obtained. The SXES and SXAS curves are normalized between their maximum intensity and ranges where their variation of intensity is negligible, so it makes sense to compare the shapes and intensities of different curves of the same spectral character for a given element in various materials.

In the photoemission spectroscopy technique (XPS) the sample is irradiated by incoming photons; electrons from a core level or the OB are ejected from the solid and their energy distribution is analysed. The spectral intensities are modulated by photoemission cross sections; these widely favour d or f states with respect to the s and p ones. The OB electronic distributions are obtained at the same time for all atomic sites and all spectral

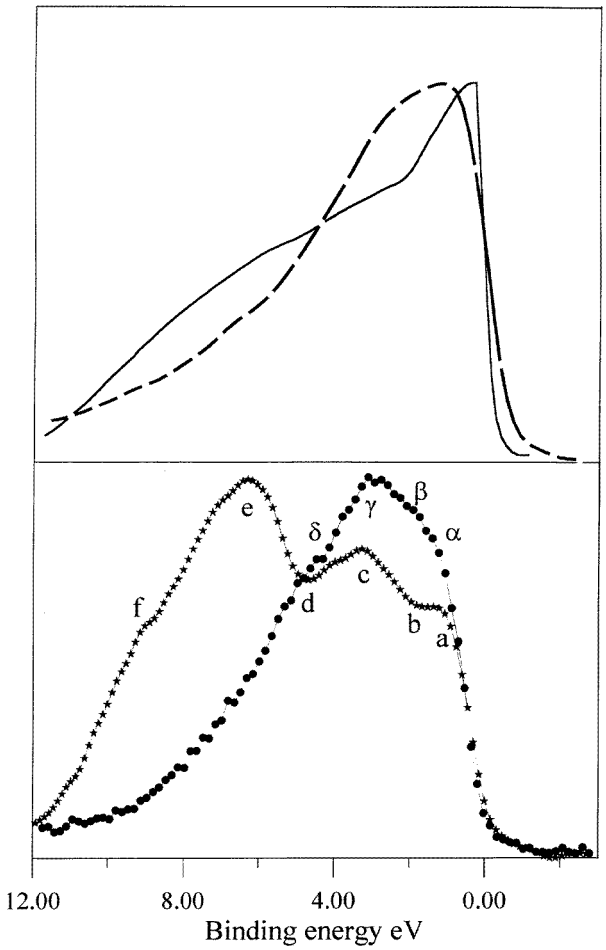

Figure 1. Upper panel, Al 3p (dashed thick line) and Al 3s, d (full thin line) spectral curves in pure fcc Al. Lower panel, Al 3p (dotted line) and Al 3s, d (starred line) spectral curves in quasicrystalline $Al_{65}Cu_{20}Ru_{15}$.

characters and core levels are obtained separately. Calibration of the binding energy scale is usually performed by referring either to the Au $4f_{7/2}$ or the C 1s level binding energies.

Description of both the OB and UB in $Al_{65}Cu_{20}Ru_{15}$ using the SXS techniques requires the probing of different partial DOSs as indicated in table 1. For OB Cu and Ru states, the spectra concern mainly the 3d and 4d state distributions respectively because the x-ray transition probabilities favour $p \rightarrow d$ transitions with respect to $p \rightarrow s$ ones; in addition, note that the s state contribution is quite faint in the pure elements (Papaconstantopoulos 1986). The different spectra are each obtained in their own x-ray transitions energy scale; thus, to gain insight into the electronic interactions, it is necessary to adjust the spectra to an absolute energy scale. This is achieved by placing E_F on the various x-ray transition energy scales owing to the measurements of the binding energies of the core levels participating in the x-ray transitions (Traverse *et al* 1988). Consequently, it is possible to adjust the different experimental partial DOSs to the binding energy scale.

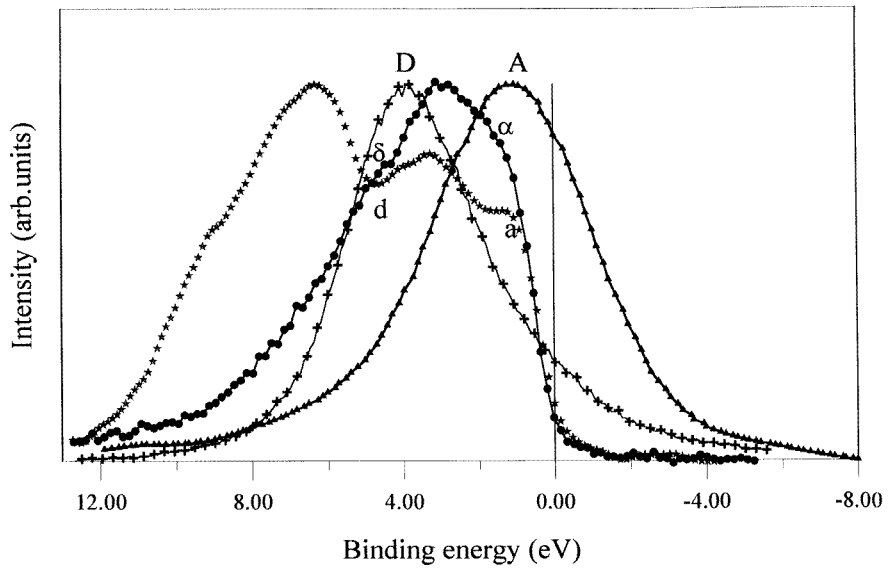

Figure 2. Occupied state distribution in quasicrystalline $Al_{65}Cu_{20}Ru_{15}$: Al 3p (dotted line), Al 3s, d (starred line), Cu 3d (line with crosses) and Ru 4d (line with triangles).

3. Experimental procedures

The SXES measurements were carried out with vacuum spectrometers fixed with bent SiO_2 $10\bar{1}0$ or KAP crystals or a grating; the energy resolutions in the investigated energy ranges are ± 0.3 eV in all cases. The spectra were excited with either incoming electrons or photons on the samples that were water cooled; the emitted photons were collected in gas flow proportional counters or with both a photocathode and a channeltron. SXES spectra of pure Al, Cu and Ru were also measured for comparison and calibration purposes.

The SXAS experiments were performed at the synchrotron facility of the Laboratoire pour l'Utilisation du Rayonnement Electromagnétique (LURE, Orsay, France). Measurements of the Cu K and Ru K absorption edges involve the transmission technique, the yield technique was applied for Al K, Ru L_{III} and Cu L_{III} edges. The Cu and Ru K absorption edges were scanned using the DCI synchrotron radiation facility (LURE) with a Si 331 channel cut single crystal (experimental station EXAFS 1: D42). The Cu L_{III}, Al K and Ru L^{III} absorption edges were probed with the Super ACO storage ring (experimental station SA 32) by means of a two-crystal monochromator equipped with either beryl $10\bar{1}0$ crystals for the Cu L_{III} edge, SiO_2 $10\bar{1}0$ slabs for the Al K edge or Si 111 plates for the Ru L_{III} edge. The instrumental resolutions of these different spectrometers are about 0.3–0.5 eV for the Super ACO equipment and about 1.4 and 6.5 eV for the energy ranges of transitions Cu K and Ru K respectively. It is also necessary to account for the intrinsic broadening due to the widths of the inner levels involved in the x-ray transitions (see table 1). Thus, finally, the energy resolutions are about 0.3 eV for Al K, 0.8 eV for Cu L_{III}, 2.0 eV for Ru L_{III}, 2.1 eV for Cu K and about 8 eV for Ru K spectra. The SXAS spectra from Al and CuO and also from $Ru_{98}Fe_2$ solid solution (prepared at the Laboratoire Mixte CNRS/Saint Gobain of Pont à Mousson) were also measured for meaningful comparison and energy calibrations.

The OB band as well as the Al $2p_{3/2}$ and Ru $3d_{5/2}$ binding energies were obtained from XPS measurements using the Mg Kα (Mg $2p_{3/2} \rightarrow 1s$) radiation; the binding energy scale was calibrated with respect to the C 1s level, taken to be equal to 285.0 eV. The $Al_{65}Cu_{20}Ru_{15}$ sample being somewhat oxidized, the Cu $2p_{3/2}$ line could not be measured with enough accuracy. However, we observe the OB XPS spectrum is dominated by a sharp peak at 4.0 ± 0.3 eV from the cut-off edge present at E_F, which we ascribed to the Cu 3d state contribution, in agreement with results from Stadnik *et al* (1994), so we could place E_F on the x-ray transition energy scale at an energy distance of 4.0 ± 0.3 eV from the maximum of the Cu Lα line. For Al, the binding energy of the 1s level could not be obtained directly. Thus, we measured the energy of the Al Kα ($2p_{3/2} \rightarrow 1s$) emission line and from the energy of Al $2p_{3/2}$ we deduced the value for the Al 1s binding energy. In the case of Ru, we did not measure directly the inner level actually involved in the probed x-ray transitions because its photoemission cross-section is rather low. We assumed a constant chemical shift of inner levels in the alloy with respect to the pure metal and we measured the Ru $3d_{5/2}$ binding energy. Finally, we locate E_F on the transition energy scales within ± 0.1 eV for Al and not better than ± 0.3–0.5 eV for the two other elements.

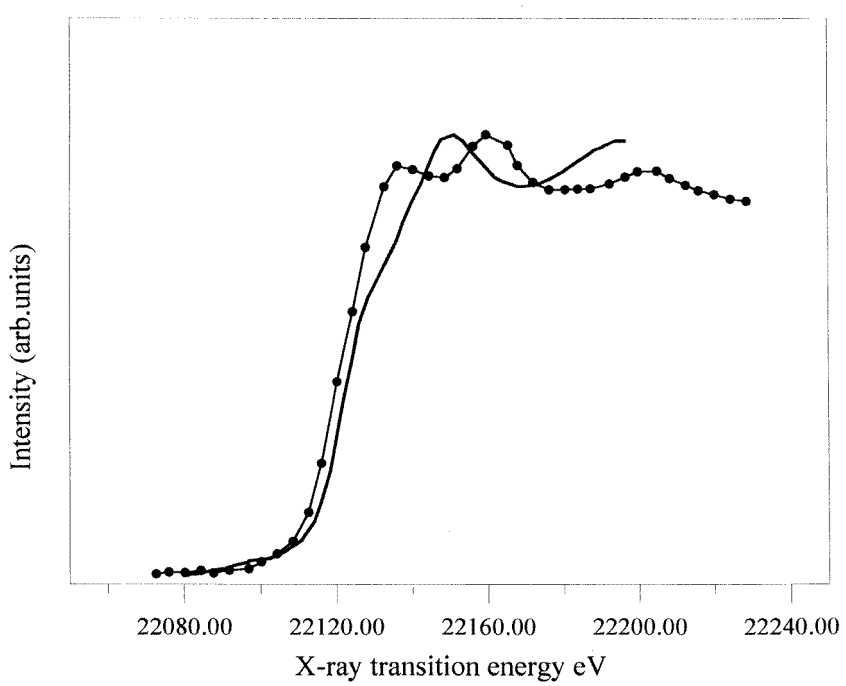

Figure 3. Ru p distribution curves in $Ru_{98}Fe_2$ solid solution (dotted line) and in quasicrystalline $Al_{65}Cu_{20}Ru_{15}$ (full line).

We produced icosahedral samples of $Al_{65}Cu_{20}Ru_{15}$ by melt spinning and subsequent annealing in evacuated sealed quartz containers at 800 °C during 7 d. The samples were characterized by powder x-ray diffraction. All the peaks could be indexed by the icosahedral phase, and the width of the peaks revealed a high structural quality. The room temperature resistivity was measured to be of the order of 1800 $\mu\Omega$ cm (Berger *et al* 1993).

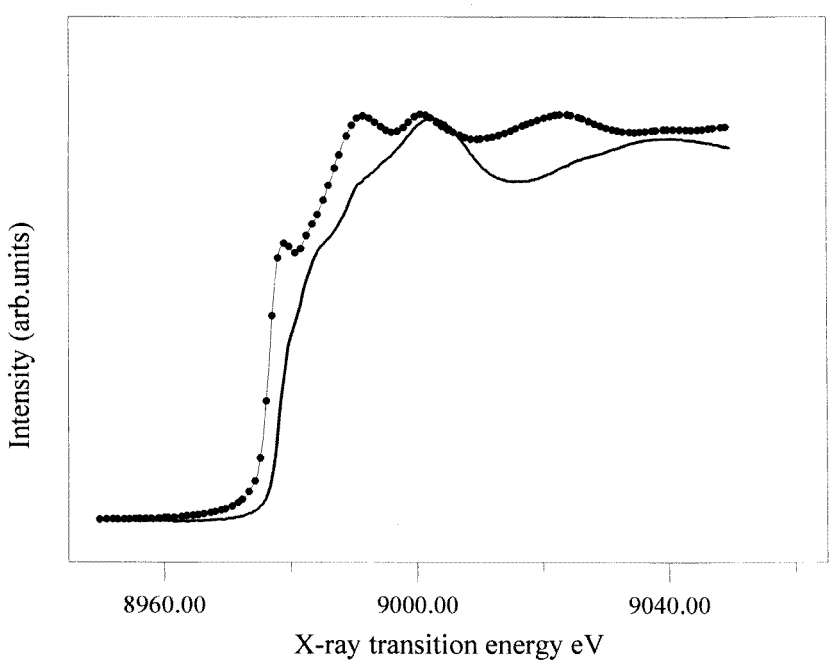

Figure 4. Cu p distribution curves in pure Cu metal (dotted line) and in quasicrystalline $Al_{65}Cu_{20}Ru_{15}$ (full line).

4. Results and discussion

The Al 3p and Al 3s, d curves for $Al_{65}Cu_{20}Ru_{15}$ are plotted in figure 1 (lower panel). Their shapes differ from those for pure fcc Al (figure 1, upper panel). In fcc Al, the Al 3p and Al 3s, d state distribution curves totally overlap, revealing strong s–p hybridization. The inflexion point of the steep Al 3p edge is exactly at E_F and its intensity is half the maximum intensity of the Al 3p sub-band. The Al 3s, d curve displays a prominent peak near E_F that is due to both the presence of d-like states and many-body effects (Nozières and de Dominicis 1969) which is characteristic of a free-electron-like metal. In $Al_{65}Cu_{20}Ru_{15}$, the Al 3p curve edge is less steep than in pure fcc Al. Two features at $E_F + 1.2 \pm 0.1$ eV and $E_F + 1.8 \pm 0.1$ eV are denoted α and β respectively; the maximum γ of the curve is at $E_F + 2.8 \pm 0.1$ eV and there is a shoulder at about $E_F + 4.1$ eV labelled δ. The edge of the Al s, d curve does not exhibit any sharp peak near E_F that indicates the free-electron model no longer works for explaining the electronic properties of this alloy. The Al 3s–d edge overlaps the Al 3p one. A peak denoted a, that coincides with α of the Al 3p curve, is followed by a short plateau until feature b which is at the same energy as shoulder β of the Al 3p curve; towards increasing binding energies, one observes a maximum denoted c in the range of peak γ of the Al 3p curve, then a minimum d in the same range as shoulder δ, a maximum denoted e at $E_F + 6.3 \pm 0.1$ eV and a faint shoulder f at about $E_F + 9$ eV. By analogy to calculations for crystalline Al–transition metal alloys (Dankházi *et al* 1993, Trambly de Laissardière *et al* 1995), we suggest the states corresponding to features (a, α) and (b, β) are Al p–d hybridized states and those corresponding to features (c, γ) and (d, δ) are s–p hybridized whereas almost s-pure states are found beyond increasing energies from

$E_F + 5$ eV. The shapes of the Cu 3d and Ru 4d distribution curves do not differ from those of the pure metals, as expected for d states, so they are not shown here.

Figure 2 shows a picture of the OB. From the overlaps between the various curves we conclude that electronic interaction exists between Al 3p–d and Ru 4d states at E_F and its vicinity and between Cu 3d and Al states in the middle of the band. The Al–Ru interaction pulls the Al states far from E_F. A pseudo-gap is formed in the Al state distribution since the distance of the Al edges to E_F taken at half maximum intensity of the Al sub-bands is 0.60 ± 0.05 eV against zero in pure Al and since the Al 3p intensity at E_F is about 13% the maximum intensity against 50% in the pure fcc Al. Also, with respect to the pure metal, the Ru 4d states are pushed closer to E_F and thus their intensity at E_F slightly increases. The Al–Cu interaction works towards splitting the Al distributions into two separate s–p-like and s-like parts and, as compared to pure Cu, significantly repels the Cu states away from E_F, which decreases the Cu 3d contribution at E_F. Within the experimental accuracy, our results for Ru 4d and Cu 3d states agree with data from XPS measurements by Nakamura and Mizutani (1994) (Ru 4d states between 1 and 2 eV and Cu 3d states at 4.3 eV from E_F) and Stadnik *et al* (1994) (Ru 4d states at 1.3 eV and Cu 3d states at 3.8 eV from E_F).

We plot in figures 3 and 4 the Ru and Cu UB p state distribution curves, respectively, for $Al_{65}Cu_{20}Ru_{15}$, $Ru_{98}Fe_2$ and pure Cu. The shapes of the curves change when going to the quasicrystal, that emphasizes notable modifications of hybridizations of states with a rather extended character when changing the local atomic environment of the Ru and Cu atoms.

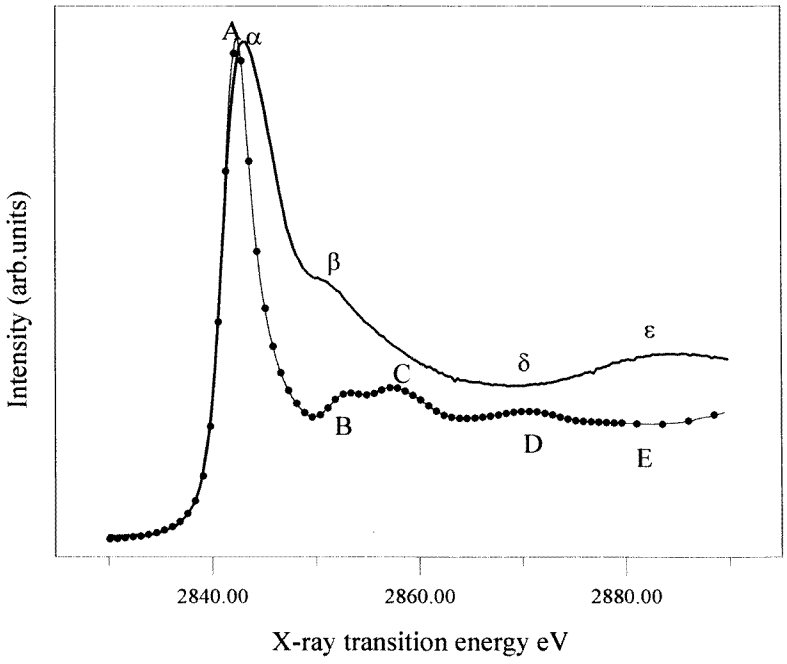

Figure 5. Ru d–s distribution curves in $Ru_{98}Fe_2$ solid solution (dotted line) and in quasicrystalline $Al_{65}Cu_{20}Ru_{15}$ (full line).

Figure 5 shows the Ru UB d–s state distribution curves in $Al_{65}Cu_{20}Ru_{15}$ and $Ru_{98}Fe_2$. The curve for $Ru_{98}Fe_2$ exhibits a sharp peak, denoted A, which following

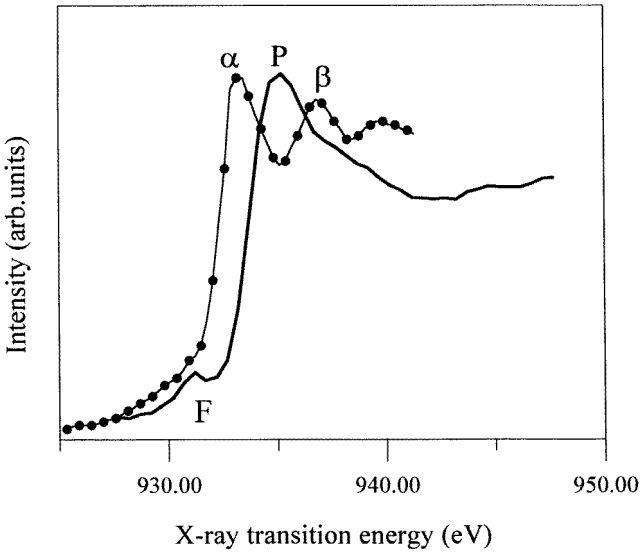

Figure 6. Cu d–s distribution curves in pure Cu metal (dotted line) and in quasicrystalline $Al_{65}Cu_{20}Ru_{15}$ (full line).

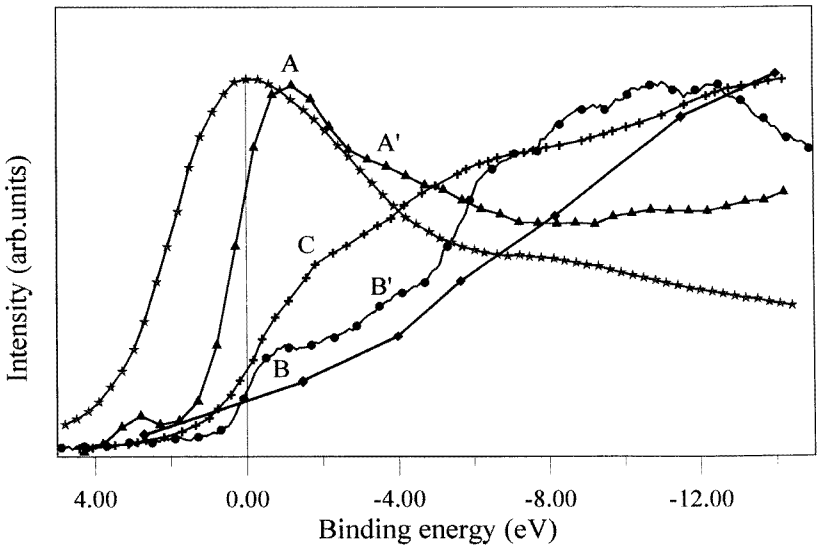

Figure 7. Unoccupied state distribution in quasicrystalline $Al_{65}Cu_{20}Ru_{15}$: Al p (dotted line), Ru d, s (starred line), Cu d, s (line with triangles), Cu p (line with crosses) and Ru p (line with squares).

Papaconstantopoulos (1986) we ascribed to d-pure states; the secondary structures, labelled B, C, D and E, correspond to s–d-like states. In $Al_{65}Cu_{20}Ru_{15}$, the curve retains a sharp peak denoted α but this one is much broader than peak A, revealing some hybridization with s states. Features marked β, δ and ε also differ from those labelled B and C, D and

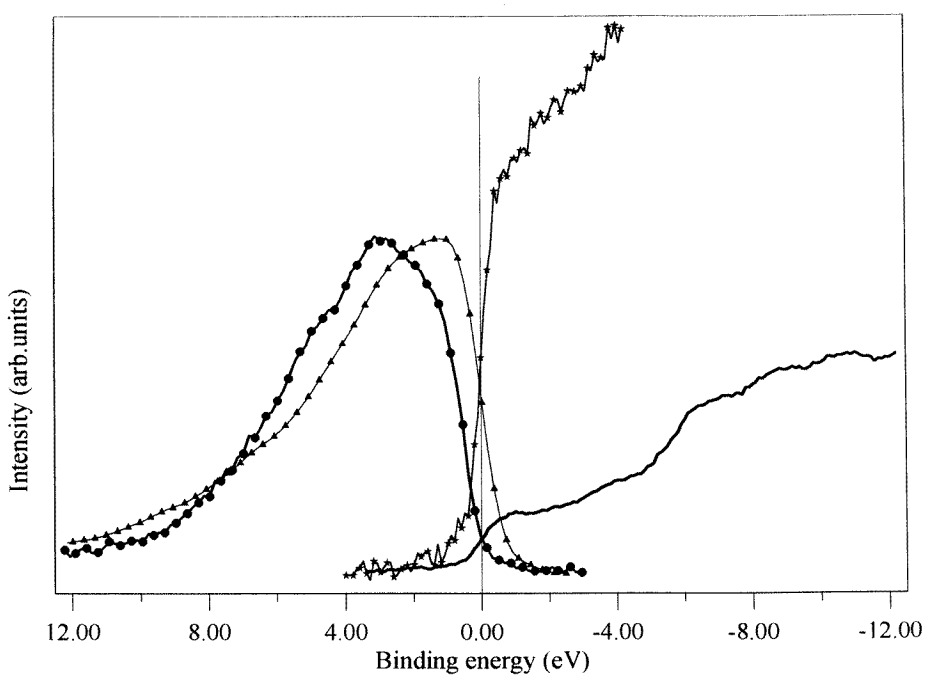

Figure 8. Occupied Al 3p and unoccupied Al p distributions in pure fcc Al (lines with triangles and with stars respectively) and in quasicrystalline $Al_{65}Cu_{20}Ru_{15}$ (dotted and full lines respectively).

E showing modifications in s–d hybridization. Such a diminishing of the d character of the first empty Ru states suggests charge transfer to Ru atoms and is thus consistent with the existence of covalent bonding in quasicrystalline $Al_{65}Cu_{20}Ru_{15}$ as pointed out by Hu *et al* (1992).

Figure 6 shows the Cu UB d–s state distribution curves in the pure metal as well as in $Al_{65}Cu_{20}Ru_{15}$. In Cu, the curve describes the $2p_{3/2} \rightarrow$s x-ray transition; it displays two peaks α and β beyond the edge consistent with the findings of Papaconstantopoulos (1986). In the alloy, the curve shows a faint 'white line' denoted P followed by a broad shoulder. This shape is reminiscent of that of absorption curves due to $2p_{3/2} \rightarrow$d state transitions (see for example the Ru L_{III} curve of $Ru_{98}Fe_2$, figure 5). This alludes to the presence in $Al_{65}Cu_{20}Ru_{15}$ of Cu unoccupied states near E_F with a slight d-like character and suggests that in this quasicrystal charge transfer may originate not only from Al atoms but also from Cu atoms, the result of which is to induce a somewhat covalent-like character of bonding in $Al_{65}Cu_{20}Ru_{15}$ (Hu *et al* 1992). This works towards the rather high resistivity of this alloy (Biggs *et al* 1990, Mizutani *et al* 1990, Nakamura and Mizutani 1994, Klein *et al* 1991, Poon 1992). Note that feature F of the curve for the quasicrystal is due to a faint contamination of the sample by CuO.

A picture of the UB is shown in figure 7. Due to the poor resolution for the Ru $2p_{3/2} \rightarrow$ UB transition, the Ru d–s curve is quite broad; however, it shows interaction near E_F with Al p states. At about 1 eV from E_F Cu d-like states (peak A) are hybridized to Cu p states (overlap of peak A and feature C) and in interaction with Al p states (bump B). At about 4 eV from E_F, Cu s-like states (feature A′) interact with Al p states (feature B′).

Then all the states of the unoccupied band are totally mixed. The Ru p-like state curve edge is very flat; this is due to the broad Ru 1s level involved in the x-ray transition. Note that we have already observed similar organization of the OB as well as UB states for other icosahedral alloys, in particular for Al–Cu–Fe (Sadoc *et al* 1993, Belin *et al* 1992, 1994, 1996).

The Al 3p and Al p distribution curves as adjusted to the Al 3p intensity at E_F are plotted in figure 8. Important depletion of Al states in the alloy is shown in the vicinity of E_F due to the formation of the pseudo-gap and near vanishing of extended Al p conduction states. As a consequence, transition of electrons to extended UB states should be somewhat less favourable in the quasicrystal than in pure fcc Al. This result is in line with previous observations for icosahedral highly resistive quasicrystalline alloys such as Al–Cu–Fe, Al–Pd–Mn and Al–Pd–Re (Belin-Ferré and Dubois 1996 and references therein).

5. Conclusion

Using SXS techniques we have investigated partial electronic distributions of states in icosahedral $Al_{65}Cu_{20}Ru_{15}$. In the OB we evidenced on the one hand Al–Ru interaction near E_F and on the other hand interaction between Al and Cu 3d states in the middle of the band. We show the formation of a rather wide pseudo-gap in the Al state distribution. For the UB, we reveal Al–Ru interaction near E_F and Al–Cu interaction beyond 1 eV from E_F and we point out a rather important depletion of Al p extended-like states. We suggest that charge transfer from Al and Cu atoms to the Ru ones together with the vanishing of the Al p states could be involved to explain the high resistivity of the $Al_{65}Cu_{20}Ru_{15}$ quasicrystalline alloy.

Acknowledgments

A M Flank and P Lagarde are acknowledged for invaluable assistance during experiments at LURE. This work has been in part supported by the Austrian Ministry of Research East-West Cooperation contract under the title ‘Soft X-ray Emission Spectroscopy of Metallic Systems’.

References

Akiyama H, Hashimoto T, Shibuya T, Edagawa K and Takeuchi S 1993 *J. Phys. Soc. Japan* **62** 639
Basov D N, Pierce F S, Volkov P, Poon S J and Timusk T 1994 *Phys. Rev. Lett.* **73** 1865
Belin E, Dankházi Z and Sadoc A 1993 *J. Non-Cryst. Solids* **156–158** 896
Belin E, Dankházi Z, Sadoc A, Calvayrac Y and Dubois J M 1994 *Europhys. Lett.* **26** 677
Belin E, Dankházi Z, Sadoc A, Calvayrac Y, Klein T and Dubois J M 1992 *J. Phys.: Condens. Matter* **4** 4459
Belin E, Dankházi Z, Sadoc A, Flank A M, Poon S J, Muller H and Kirchmayr H 1996 *Proc. 5th Int. Conf. on Quasicrystals* ed C Janot and R Mosseri (Singapore: World Scientific) pp 435–8
Belin-Ferré E and Dubois J M 1996 *J. Mat. Res.* submitted
Berger C, Belin E and Mayou D 1993 *Ann. Chim.* **18** 485
Biggs B D, Poon J S and Munirathnam N R 1990 *Phys. Rev. Lett.* **65** 2700
Dankházi Z, Trambly de Laissardière G, Nguyen Manh D, Belin E and Mayou D J 1993 *J. Phys.: Condens. Matter* **5** 3339
Fujiwara T 1993 *J. Non-Cryst. Solids* **153–154** 390
Fujiwara T, Yamamoto S and Trambly de Laissardière G 1993 *Phys. Rev. Lett.* **71** 4166
Fujiwara T and Yokokawa T 1991 *Phys. Rev. Lett.* **63** 333
Hippert F, Kandel L, Calvayrac Y and Dubost B 1992 *Phys. Rev. Lett.* **69** 2086
Hu R, Egami T, Tsai A P, Inoue A and Masumoto T 1992 *Phys. Rev.* B **46** 6105

Klein T, Berger C, Mayou D and Cyrot-Lackmann F 1991 *Phys. Rev. Lett.* **66** 2907
Krajci M and Hafner J 1993 *J. Non-Cryst. Solids* **156–158** 887
Krajci M, Windisch M, Hafner J, Kresse G and Mihalkovic M 1995 *Phys. Rev.* B **51** 17 335
Krause M O and Oliver J H 1979 *J. Phys. Chem. Ref. Data* **8** 329
Lanco P, Klein T, Berger C, Cyrot-Lackmann F, Fourcaudot G and Sulpice A 1992 *Europhys. Lett.* **18** 227
Mizutani U, Sakabe Y, Shibuya T, Kishi K, Kimura K and Takeuchi S 1990 *J. Phys.: Condens. Matter* **2** 6169
Mori M, Matsuo S, Ishimasa T, Matsuura T, Kamiya K, Inokuchi H and Matsukawa T 1991 *J. Phys.: Condens. Matter* **3** 767
Nakamura Y and Mizutani U 1994 *Mater. Sci. Eng.* A **181–182** 790
Nozières P and de Dominicis C T 1969 *Phys. Rev.* **178** 6105
Papaconstantopoulos D A 1986 *Handbook of the Band Structures of Elemental Solids* (New York: Plenum) pp 119, 122 for Cu; pp 149, 151 for Ru
Pierce F S, Poon S J and Guo Q 1993 *Science* **261** 737
Poon S J 1992 *Adv. Phys.* **41** 303
Poon S J, Pierce F S, Guo Q and Volkov P 1996 *Proc. 5th Int. Conf. on Quasicrystals* ed C Janot and R Mosseri (Singapore: World Scientific)
Sadoc A, Belin E, Dankházi Z and Flank A M 1993 *J. Non-Cryst. Solids* **153–154** 338
Stadnik Z M and Stroink G 1993 *Phys. Rev.* B **47** 100
Stadnik Z, Zhang G W, Tsai A P and Inoue A 1994 *J. Phys.: Condens. Matter* **6** 1097
Tamura R, Waseda A, Kimura K and Ino H 1994 *Mater. Sci. Eng.* A **182** 790; 1994 *Phys. Rev.* B **50** 9640
Trambly de Laissardière G, Dankházi Z, Belin E, Sadoc A, Nguyen Manh D, Mayou D, Keegan M A and Papaconstantopoulos D A 1995 *Phys. Rev.* B **51** 14 035
Traverse A, Dumoulin L, Belin E and Sénémaud C 1988 *Quasicrystalline Materials* ed C Janot and J M Dubois (Singapore: World Scientific) p 399